HHS Public Access

Author manuscript

Biochem Cell Biol. Author manuscript; available in PMC 2015 August 01.

Published in final edited form as:

Biochem Cell Biol. 2015 August ; 93(4): 343–350. doi:10.1139/bcb-2015-0009.

Anti-CD20 single chain variable antibody fragment–apolipoprotein A-I chimera containing nanodisks promote targeted bioactive agent delivery to CD20-positive lymphomas

Natasha M. Crosby[*],
Lypro Biosciences Inc., 1236 Hawthorne St. Alameda, CA 94501, USA

Mistuni Ghosh[*],
Children's Hospital Oakland Research Institute, 5700 Martin Luther King Jr. Way, Oakland, CA 94609, USA

Betty Su,
Children's Hospital Oakland Research Institute, 5700 Martin Luther King Jr. Way, Oakland, CA 94609, USA

Jennifer A. Beckstead,
Children's Hospital Oakland Research Institute, 5700 Martin Luther King Jr. Way, Oakland, CA 94609, USA

Ayako Kamei,
Children's Hospital Oakland Research Institute, 5700 Martin Luther King Jr. Way, Oakland, CA 94609, USA

Jens B. Simonsen,
Children's Hospital Oakland Research Institute, 5700 Martin Luther King Jr. Way, Oakland, CA 94609, USA

Bing Luo,
Lypro Biosciences Inc., 1236 Hawthorne St. Alameda, CA 94501, USA

Leo I. Gordon,
Division of Hematology/Oncology, Department of Medicine, Northwestern University Feinberg School of Medicine, Chicago, IL 60611, USA

Trudy M. Forte, and
Lypro Biosciences Inc., 1236 Hawthorne St. Alameda, CA 94501, USA; Children's Hospital Oakland Research Institute, 5700 Martin Luther King Jr. Way, Oakland, CA 94609, USA

Robert O. Ryan
Children's Hospital Oakland Research Institute, 5700 Martin Luther King Jr. Way, Oakland, CA 94609, USA

Abstract

Corresponding author: Robert O. Ryan (rryan@chori.org).
[*]These authors contributed equally.

A fusion protein comprising an α-CD20 single chain variable fragment (scFv) antibody, a spacer peptide, and human apolipoprotein (apo) A-I was constructed and expressed in *Escherichia coli*. The lipid interaction properties intrinsic to apoA-I as well as the antigen recognition properties of the scFv were retained by the chimera. scFv•apoA-I was formulated into nanoscale reconstituted high-density lipoprotein particles (termed nanodisks; ND) and incubated with cultured cells. α-CD20 scFv•apoA-I ND bound to CD20-positive non-Hodgkins lymphoma (NHL) cells (Ramos and Granta) but not to CD20-negative T lymphocytes (i.e., Jurkat). Binding to NHL cells was partially inhibited by pre-incubation with rituximab, a monoclonal antibody directed against CD20. Confocal fluorescence microscopy analysis of Granta cells following incubation with α-CD20 scFv•apoA-I ND formulated with the intrinsically fluorescent hydrophobic polyphenol, curcumin, revealed α-CD20 scFv•apoA-I localizes to the cell surface, while curcumin off-loads and gains entry to the cell. Compared to control incubations, viability of cultured NHL cells was decreased upon incubation with α-CD20 scFv•apoA-I ND harboring curcumin. Thus, formulation of curcumin ND with α-CD20 scFv•apoA-I as the scaffold component confers cell targeting and enhanced bioactive agent delivery, providing a strategy to minimize toxicity associated with chemotherapeutic agents.

Keywords

single chain variable antibody fragment; CD20; nanodisk; apolipoprotein A-I; curcumin; non-Hodgkin’s lymphoma; confocal fluorescence microscopy

Introduction

A subset of reconstituted high-density lipoproteins (rHDL) includes self-assembled disk-shaped phospholipid bilayers, whose perimeter is stabilized by a protein scaffold. In recent years rHDL have been repurposed for applications well beyond lipoprotein metabolism (Ryan 2008). One such application involves the incorporation of small hydrophobic bioactive agents (Ryan 2010). To distinguish rHDL enriched with an exogenous bioactive agent from classical phospholipid-apolipoprotein assemblies, the term nanodisk (ND) is used. Included among the small, hydrophobic bioactive agents that have been solubilized in ND are the polyene antifungal, amphotericin B (Oda et al. 2006; Burgess et al. 2010), the isoprenoid, all-trans retinoic acid (Redmond et al. 2007; Singh et al. 2010), the anti-oxidant polyphenol, curcumin (Ghosh et al. 2011; Singh et al. 2011), and the cholesterol biosynthesis inhibitor, simvastatin (Duivenvoorden et al. 2014).

A limitation of existing ND technology for anti-cancer applications relates to the risk of nonspecific cytotoxic effects following systemic administration of a bioactive agent containing ND. To confer cell/tissue specificity, it may be possible to engineer the protein scaffold component of ND, usually a member of the class of exchangeable apolipoproteins (apo). An example of this concept is the construction of an apolipoprotein–single chain variable antibody fragment (scFv) chimera. An scFv is preferred over a Fab fragment or intact antibody for this purpose, because an scFv is wholly encoded by a single nucleotide sequence (Hagemeyer et al. 2009). In fact, experimental validation of this general concept has been obtained by construction of a chimera composed of recombinant human apoA-I

and an α-vimentin scFv (Iovannisci et al. 2009). Building on this strategy, we sought to employ an scFv that would target a unique surface antigen expressed on a cancer cell population. Criteria for selection of the candidate cell surface antigen includes (*i*) well-characterized tissue-specific distribution of the antigen,(*ii*) the therapeutic relevance of the target cell population, and (*iii*) the need for improved therapy options.

Among cell surface antigen candidates considered, the choice to focus on CD20 was based on the availability of an scFv clone with known CD20 antigen recognition properties (Shan et al. 1999), the availability of a monoclonal antibody (mAb) that recognizes the same antigen (i.e., rituximab; (Press et al. 1995; Maloney et al. 1997; Scott 1998), and the need for new strategies to treat B cell lymphomas (Gordon et al. 2014). CD20 is a membrane-spanning glycosylated phosphoprotein expressed on the surface of B-cells, but not T lymphocytes (Tedder and Engel 1994). Indeed, CD20 is expressed on large B cell lymphomas (BCL), mantle cell lymphoma (MCL), hairy cell leukemia, and B cell chronic lymphocytic leukemia.

In the present study, construction and characterization of a novel recombinant α-CD20 scFv•apoA-I chimera is described. The purified fusion protein (α-CD20 scFv•apoA-I) was formulated with phospholipid and lipophilic bioactive agent (i.e., curcumin) to generate ND (α-CD20 scFv•apoA-I ND) that target cells expressing CD20. When combined with the inherent bioactive agent loading capacity of ND, α-CD20 scFv•apoA-I ND provides a means to enhance therapeutic efficacy by targeting cell/tissue-specific interactions. The results reveal that curcumin-α-CD20 scFv•apoA-I ND target CD20-positive lymphoma cells, inducing cell death commensurate with curcumin delivery.

Materials and methods

Cell lines and reagents

Ramos (Burkitt's B cell lymphoma) and Jurkat (T-cell lymphoma) cells were purchased from ATCC; Granta (Mantle cell lymphoma) cells were kindly provided by Dr. Steven Bernstein (University of Rochester, New York, USA). FITC-goat anti-human apoA-I was purchased from Abcam (Cambridge, Massachusetts, USA). Hoechst 33342 stain was purchased from Life Technologies Corp. (Carlsbad, California, USA). Alexa Fluor 680 labeled anti-goat secondary antibody was purchased from Li-Cor Biosciences (Lincoln, Nebraska, USA). Anti-fade mounting medium was from Vector Laboratories (Burlingame, California, USA). SDS-PAGE gels (10%) were from Bio Rad (Hercules, California, USA).

Cell culture and incubations

Granta and Jurkat cells were cultured in RPMI-1640 containing 10% fetal bovine serum (FBS) in the presence of glutamine. Ramos cells were cultured in RPMI-1640 containing 10% FBS and 1% sodium pyruvate, in the presence of glutamine. All cells were passaged every 2–3 days. Cell viability was measured by trypan blue exclusion.

cDNA construction

The α-CD20 scFv•apoA-I cDNA construct was generated from an α-CD20 scFv cDNA kindly provided by Dr. Oliver Press (University of Washington). A polylinker was introduced at the 3′ terminus, in addition to two restriction sites to allow joining of the scFv cDNA to a cDNA encoding human apoA-I. A 3′ terminal His-tag encoding sequence was introduced to facilitate downstream processing of the expressed fusion protein. Briefly, *Nde*I and *Cla*I restriction sites were introduced into the 5′ and 3′ terminal ends, respectively, of the α-CD20 scFv nucleotide sequence by gene amplification. The reverse primer also included nucleotide sequences encoding a $gly_{(4)}$-ser-$gly_{(4)}$-ser peptide linker to serve as a spacer between the α-CD20 scFv and apoA-I components of the fusion protein. The amplified α-CD20 scFv gene product was double digested with *Nde*I and *Cla*I (New England Biolabs) and ligated into the *Nde*I/*Cla*I double digest cloning site located at the 5′ terminus of a modified Bluescript KS(+) plasmid (Ryan, Forte, and Oda 2003). The resulting α-CD20 scFv•apoA-I cDNA was released from the plasmid vector by *Nde*I/*Hind*III double digestion and ligated into the *Nde*I/*Hind*III polylinker region of pET41b(+) expression vector (Novagen) containing an in-frame 3′ terminal His-tag. The final gene construct encoded a chimeric protein containing the alkaline phosphatase A (PhoA) signal peptide, α-CD20 scFv, $gly_{(4)}$-ser-$gly_{(4)}$-ser peptide linker, apoA-I and His-tag as follows: NH_2-PhoA•α-CD20 scFv•linker•apoA-I•His-tag-COOH, hereafter referred to as α-CD20 scFv•apoA-I. Conditions established for culture, expression, and isolation of recombinant human apoA-I from *Escherichia coli* (Ryan, Forte, and Oda 2003) were adapted for production of the α-CD20 scFv•apoA-I. Highly purified recombinant fusion protein was produced with a yield of ~10 mg/L culture medium.

Preparation of ND

ND were formulated as previously described (Ryan 2008) using apoA-I or α-CD20 scFv•apoA-I as the scaffold component. Briefly, dimyristoylphosphatidylcholine (DMPC), deposited as a thin film on the vessel wall by solvent evaporation under N_2 gas, was dispersed with phosphate buffered saline (PBS) containing a scaffold component at a lipid/protein (*w*/*w*) ratio of 2.5:1 (human apoA-I) or 2.5:2 (α-CD20 scFv•apoA-I) and bath-sonicated for 5 min or until the solution cleared. Where specified, curcumin-containing α-CD20 scFv•apoA-I ND were formulated as described by Ghosh et al. (2011). In all cases, ND were dialyzed against PBS and stored at 4 °C until use.

Electron microscopy

Negative stain (2% potassium phosphotungstate, pH 6.5) electron microscopy was performed as previously described (Burgess et al. 2013). Grids were examined at 80 kV in a JEM-1230 electron microscope (JEOL USA, Peabody, Massachusetts, USA). Particle size measurements were made using an ocular micrometer and 100 particles per sample were measured.

Flow cytometry of cells incubated with apoA-I ND and α-CD20 scFv•apoA-I ND

The interaction of apoA-I ND or α-CD20 scFv•apoA-I ND with cell surfaces was examined as described by Shan et al. (1999). Briefly, cell pellets from Ramos, Granta, and Jurkat cells

were re-suspended in RPMI + 5% FBS media. Cells (1 mL final volume) were incubated with a specified ND at 50 μg α-CD20 scFv•apoA-I protein/mL (α-CD20 scFv•apoA-I ND) or 25 μg apoA-I protein/ml (apoA-I ND) for 1 h at 37 °C. Cells were washed twice (12 000*g* for 3 min), re-suspended in media (1 mL) prior to incubation with FITC-goat anti-human apoA-I (5 μg) on ice for 30 min. Following incubation, the cells were washed and re-suspended in 600 μL ice-cold media. Cell associated fluorescence was measured by flow cytometry using BD Biosciences FacsCalibur. Markers were set using control incubations of cells with PBS to designate FITC-goat α-apoA-I-negative cells (M1) and FITC-goat α-apoA-I-positive cells (M2). The percentage of FITC-goat α-apoA-I positive cells is reported as the percentage of cells in M2.

Cell incubations with rituximab

Granta and Ramos cells were pelleted and re-suspended in RPMI media + 5% FBS. The cells (1 mL final volume) were incubated in the presence or absence of a 10-fold molar excess of rituximab over α-CD20 scFv•apoA-I for 45 min at 4 °C. Following incubation, the cells were washed to remove unbound α-CD20 scFv•apoA-I ND and rituximab. FITC-goat anti-human apoA-I (5 μg) was added, and the cells were incubated for 30 min on ice. After two washes, the cells were re-suspended in 600 μL ice-cold media and cell-associated fluorescence was measured by flow cytometry.

Confocal fluorescence microscopy studies

Granta cells (2×10^5) were incubated with 20 μmol/L curcumin-loaded α-CD20 scFv•apoA-I ND for 1 h at 37 °C. After incubation, the cells were washed with PBS to remove excess unbound curcumin-α-CD20 scFv•apoA-I ND and fixed with 4% paraformaldehyde (prepared in PBS containing 0.03 mol/L sucrose) for 10 min at 4 °C. To visualize the α-CD20 scFv•apoA-I fusion protein, fixed cells were permeabilized with 0.2% saponin in PBS + 0.03 mol/L sucrose + 1% BSA (bovine serum albumin) for 5 min at room temperature followed by 2 h incubation with goat anti-apoA-I primary (1:150 dilution) and a 1 h incubation with Alexa Fluor 680 labeled anti-goat secondary antibody (1:100 dilution). Curcumin localization was determined by excitation of the argon-ion laser at 488 nm with emission recorded in the green spectral region (493–630 nm). Hoechst 33342 was employed as a nuclear stain. Cells were deposited onto a glass slide, covered with a glass coverslip, sealed with nail polish, and visualized at 63× with the Zeiss LSM710 confocal microscope.

Effect of curcumin-loaded α-CD20 scFv•apoA-I ND on cell viability of B cell lymphoma

Cells were plated in 96-well culture plates (25 000 cells per 100 μL per well), and after 24 h, empty α-CD20 scFv•apoA-I ND (0 μmol/L curcumin) or loaded curcumin-α-CD20 scFv•apoA-I ND were added to the wells (5 and 20 μmol/L curcumin). After 48 h incubation, a CellTiter 96 AQueous Non-Radioactive Cell Proliferation Assay (Promega, Madison, Wisconsin, USA) was performed. Briefly, cells were incubated with MTT (3-[4,5-dimethylthiazol-2-yl]-2,5-diphenyltetrazolium bromide) for 2 h at 37 °C, followed by the addition of solubilization buffer for 1 h. Subsequently, well contents were mixed and 100 μL transferred to a fresh plate. Absorbance was read at 570 nm. Values expressed are the mean ± SEM ($n = 4$) percent cell viability relative to untreated cells.

Statistical analysis

Statistical analyses were performed using the Student's *t*-test (GraphPad Prism version 6.0, San Diego, California, USA). Data are shown as mean ± SEM.

Results

Construction and characterization of α-CD20 scFv•apoA-I fusion protein

To confer a targeting feature to ND, the scaffold component was engineered as an α-CD20 scFv•apoA-I fusion protein using recombinant DNA technology. The α-CD20 scFv selected for study was originally generated from a monoclonal antibody directed against the CD20 antigen on B lymphocytes, and its specificity has been established (Shan et al. 1999). The schematic in Fig. 1 (left) depicts the design strategy employed, wherein the N terminus of the fusion protein contains the cleavable PhoA sequence adjacent to the α-CD20 scFv, a 10 amino acid spacer followed by human apoA-I and a C-terminal His-Tag sequence. The expectation is that the chimera will not only possess the antigen recognition properties of the scFv but also the ND formation activity of apoA-I. A model depicting the organization of components of α-CD20 scFv•apoA-I ND is presented in Fig. 1. SDS-PAGE immunoblot analysis provided evidence of fusion protein expression in *E. coli* (Fig. 1 right). Whereas recombinant apoA-I has the expected MW of ~28 kDa, the α-CD20 scFv•apoA-I fusion protein has a MW of 54 KDa.

A characteristic property of apoA-I is its intrinsic ability to solubilize certain phospholipid dispersions, converting them into nanoscale disk-shaped lipid bilayers (Ryan 2008). In a similar manner, α-CD20 scFv•apoA-I fusion protein efficiently solubilized an aqueous dispersion of DMPC, as seen by negative stain electron microscopy (Fig. 2A). The empty ND (no drug) consisted of discoidal particles that are seen "on edge" as stacked discs or "en face" as round particles (mean particle diameter 28 ± 7 nm, $n = 100$). Curcumin-loaded α-CD20 scFv•apoA-I ND (Fig. 2*b*) consisted of larger particles having a mean particle diameter of 59 ± 11 nm ($n = 100$).

FACS Analysis of α-CD20 scFv•apoA-I ND cell interactions

Having shown that α-CD20 scFv•apoA-I fusion protein possesses nanodisk-forming activity, the ability of α-CD20 scFv•apoA-I ND to recognize and bind cell-associated CD20 antigen was investigated. Experiments were conducted with three cell lines, Ramos, Granta, and Jurkat. The former two lines represent NHLs that are known to express CD20 at their cell surface. The latter (Jurkat) is a T lymphocyte cell line that does not express CD20. The interaction of α-CD20 scFv•apoA-I ND with each of these cells lines was measured by FACS using a fluorescent-tagged antibody directed against the apoA-I component of the fusion protein (Fig. 3). The data show that treatment of Ramos cells with PBS or apoA-I ND failed to enhance cell associated fluorescence. By contrast, a prominent increase in cell-associated fluorescence occurred upon incubation of Ramos or Granta cells with α-CD20 scFv•apoA-I ND [86 ± 10% for Ramos ($n = 3$); 98 ± 1% for Granta ($n = 2$)]. By contrast, little binding was detected with Jurkat cells (6 ± 3%; $n = 3$), confirming the absence of CD20 on these cells. These data provide evidence that ND binding to Ramos and Granta

cells is not due to the apoA-I component of α-CD20 scFv•apoA-I fusion protein, but rather requires the α-CD20 scFv moiety.

Competition studies with rituximab

The monoclonal antibody, rituximab, recognizes CD20 and is widely used as a therapeutic agent in treatment of lymphoma (Scott 1998). When Ramos or Granta cells were pre-incubated with rituximab, decreased binding of α-CD20 scFv•apoA-I ND was observed (Fig. 4). As seen in the histogram, rituximab induced a 33% ($p \leq 0.001$) reduction in α-CD20 scFv•apoA-I ND binding to Ramos cells and 24% ($p \leq 0.014$) reduction in binding to Granta cells. The lack of complete inhibition is likely due to differences in epitope recognition by the α-CD20 scFv versus rituximab (Polyak and Deans 2002). Taken together, the results support the conclusion that α-CD20 scFv•apoA-I ND recognize and interact with the CD20 antigen on NHL cells.

Confocal fluorescence microscopy of α-CD20 scFv•apoA-I ND interaction with target cells

To examine the nature of α-CD20 scFv•apoA-I ND interaction with cells as well as the potential utility of these particles to serve as a vehicle for drug delivery, αCD20 scFv•apoA-I ND were formulated with the hydrophobic polyphenol, curcumin. Curcumin is an intrinsically fluorescent molecule that is postulated to intercalate between phospholipids in the bilayer of ND particles, as depicted in Fig. 1. Among numerous biological properties attributed to curcumin (Gupta et al. 2011) is a pro-apoptotic effect on cultured lymphoma cells (Singh et al. 2011), (Teeling et al. 2006). When Granta cells were incubated with curcumin-α-CD20 scFv•apoA-I ND for 1 h at 37 °C, confocal fluorescence microscopy was performed to examine the cellular location of the α-CD20scFv•apoA-I scaffold component and the bioactive agent, curcumin (Fig. 5). Whereas curcumin fluorescence showed a diffuse cytoplasmic distribution (Fig. 5*a*, green fluorescence), the α-CD20 scFv•apoA-I component was largely retained at the cell surface (Fig. 5*b*, red fluorescence). The images suggest that α-CD20 scFv•apoA-I ND binding to CD20 at the cell surface promotes curcumin dissociation and entry into these cells. A merged image (Fig. 5*c*) reveals that a small portion of the curcumin payload remains at the cell surface along with the bulk of the α-CD20 scFv•apoA-I fusion protein (yellow fluorescence). This finding is consistent with the fact that CD20, unlike many other surface antigens and receptors, is not internalized (Gordon et al. 2014). In control experiments with CD20-negative Jurkat cells, no α-CD20 scFv•apoA-I ND binding or internalized curcumin fluorescence was detected (Fig. 5*d*).

Effect of curcumin-α-CD20 scFv•apoA-I ND on cell viability

The effect of curcumin-α-CD20 scFv•apoA-I ND on cultured B cell lymphoma viability was investigated in Granta cells and Ramos cells. When treated for 48 h with α-CD20 scFv•apoA-I ND lacking curcumin, both Granta and Ramos cells showed modest reductions (~30%) in cell viability compared to cells treated with PBS (Fig. 6). At 5 μmol/L curcumin, a significant decline (65 ± 10%, $p \leq 0.001$) in cell viability, compared to empty α-CD20 scFv•apoA-I ND, was observed in Ramos, but not Granta, cells. At 20 μmol/L curcumin, Ramos cells were highly responsive, with a >90% reduction in cell viability. Granta cells, on the other hand, displayed less cell death (51 ± 4%, $p \leq 0.001$) at this curcumin concentration.

The data suggest that α-CD20 scFv•apoA-I ND solubilize curcumin and promote its cellular uptake via interaction with CD20. The observation that the two cell lines investigated show differential sensitivity to the drug, in terms of its effect on cell viability, is likely due to cell-specific effects of curcumin. Furthermore, the apparent ~30% cytotoxicity observed in control experiments with empty α-CD20 scFv•apoA-I ND suggests that scFv binding to the CD20 antigen alone elicits an effect.

Discussion

The present study demonstrates the feasibility of using recombinant α-CD20 scFv•apoA-I fusion protein to produce a ND that promotes bioactive agent delivery to CD20-positive NHL cells. This study builds on previous work showing that α-CD20 scFv recognizes the CD20 antigen on the surface of B lymphocytes (Shan et al. 1999). The potential application of this binding interaction for targeted delivery of drugs to tumor cells is attractive, because it is anticipated to reduce or eliminate non-specific cell toxicity. A recent study analyzing the effect of nanoparticle morphology on the efficiency of drug delivery in cultured epithelial cells concluded that nanorods are less potent in drug delivery than nanodisks, while both these morphologies are superior to nanospheres (Agarwal et al. 2013). Taking advantage of this feature, α-CD20 scFv•apoA-I fusion protein was formulated into disk-shaped nanoparticles (i.e., ND). The α-CD20 scFv•apoA-I component of the product ND functions as a scaffold that circumscribes the perimeter of a disk-shaped phospholipid bilayer. This structural matrix provides an environment into which hydrophobic bioactive agents can be intercalated (Ryan 2008). In the present formulation, it is envisioned that the apoA-I portion of the fusion protein contacts the edge of the ND bilayer, while the α-CD20 scFv portion is exposed to the aqueous environment (see Fig. 1). As such, the scFv will be exposed to the aqueous milieu while adopting a functional conformation capable of antigen recognition.

FACS analysis demonstrated that α-CD20 scFv•apoA-I ND display binding specificity for CD20 on both MCL (Granta) and BCL (Ramos) cells in culture, whereas CD20-negative Jurkat cells showed no binding. The latter observation suggests that discoidal morphology alone is insufficient to support cell binding in the absence of CD20. Flow cytometry studies also revealed that the α-CD20 scFv component of the fusion protein is required for cell surface CD20 recognition. On the other hand, ND formulated with apoA-I showed virtually no binding to Jurkat cells, reinforcing the conclusion that binding is specific for the α-CD20 scFv moiety.

Discovery that the α-CD20 mAb, rituximab, is efficacious in treatment of NHL (Maloney et al. 1997) raised awareness of the potential utility of targeted anti-cancer therapy. Investigations with antibody-drug conjugates (ADC) have led to the concept that combining mAbs with small molecule chemotherapeutic drugs has potential for synergy (Gerber et al. 2013; Lianos et al. 2014). Although ADC provides an important means of delivering drugs to tumor cells, only a limited number of drug molecules can be conjugated to a given mAb.

Curcumin is a natural occurring polyphenol that has been shown in cell studies to be beneficial in treating hematological cancers (Singh et al. 2011; Shishodia et al. 2005;

Hussain et al. 2008) as well as other cancers (Shankar et al. 2007; Ghosh and Ryan 2014). It is informative that, whereas curcumin was taken up by CD20-positive cells, the ND scaffold component remained at the cell surface, presumably via interaction with CD20. Indeed, 30 or more molecules of curcumin can be incorporated into each ~60 nm α-CD20 scFv•apoA-I ND, making this an attractive bioactive agent delivery vehicle. One can speculate, that when the curcumin-α-CD20 scFv•apoA-I ND binds to CD20 on the surface of a target cell, close proximity of the particle to the cell membrane promotes bioactive agent interaction with the membrane lipids, with subsequent transit into the cytoplasmic compartment. Indeed, it has been demonstrated that exposure of CD20 to rituximab correlates with translocation of the protein to detergent insoluble lipid rafts (Deans et al. 2002; Cragg et al. 2003). Such an itinerary can favor diffusion of hydrophobic bioactive agents into the cell. Consistent with this interpretation, confocal microscopy studies with curcumin-loaded α-CD20 scFv•apoA-I ND revealed that the fusion protein component of the ND remains at the cell surface. Thus, curcumin-α-CD20 scFv•apoA-I ND facilitates intracellular delivery of curcumin. At the same time, it is recognized that uptake of curcumin in this cultured cell system is not solely dependent upon CD20 binding. Indeed, apoA-I curcumin ND have been shown to be cytotoxic to lymphoma cells in culture (Singh et al. 2011) and “free” curcumin is taken up by cultured glioblastoma multiforme cells (Ghosh and Ryan 2014). As such, it is conceivable that one or more alternate receptors, such as the scavenger receptor class B type I (Shen et al. 2014), contribute to the observed uptake/cytotoxicity in this system. Thus, although binding to CD20 has been achieved with α-CD20 scFv•apoA-I ND, the contribution of this interaction to cellular uptake of curcumin, compared to other potential mechanisms, remains to be fully elucidated.

In summary, we show the feasibility of formulating targeted scFv•apoA-I ND that have the ability to deliver a hydrophobic bioactive agent to α-CD20-positive tumor cells. Whereas we took advantage of the intrinsic fluorescence properties of curcumin to evaluate cellular uptake in the present study, it is likely that incorporating more potent drugs into targeted ND would produce more significant cytotoxic effects. It is also anticipated that ND can be formulated to target other tumor-specific cell surface proteins and (or) receptors, wherein the drug load is tailored to specific dysfunctional molecular pathways that lead to tumor proliferation.

Acknowledgments

We wish to thank Jianhui Zho for helpful discussions related to periplasmic expression. Supported by grants from NIH: R37 HL64159 (ROR) and 1R43CA141904 (TMF). The content is solely the responsibility of the authors and does not represent the official views of NIH. JBS acknowledges support from the Danish VKR and IMK Almene Foundations.

References

Agarwal R, Singh V, Jurney P, Shi L, Sreenivasan SV, Roy K. Mammalian cells preferentially internalize hydrogel nanodiscs over nanorods and use shape-specific uptake mechanisms. Proc Natl Acad Sci USA. 2013; 110(43):17247–17252.10.1073/pnas.1305000110 [PubMed: 24101456]

Burgess BL, Cavigiolio G, Fannucchi MV, Illek B, Forte TM, Oda MN. A phospholipid-apolipoprotein A-I nanoparticle containing amphotericin B as a drug delivery platform with cell membrane protective properties. Int J Pharm. 2010; 399(1–2):148–155.10.1016/j.ijpharm.2010.07.057 [PubMed: 20696226]

Burgess BL, He Y, Baker MM, Luo B, Carroll SF, Forte TM, Oda MN. Nanodisk containing super aggregated amphotericin B: A high therapeutic index antifungal formulation with enhanced potency. Int J Nanomedicine. 2013; 8:4733–4743.10.2147/IJN.S50113 [PubMed: 24379661]

Cragg MS, Morgan SM, Chan HT, Morgan BP, Filatov AV, Johnson PW, et al. Complement-mediated lysis by anti-CD20 mAb correlates with segregation into lipid rafts. Blood. 2003; 101(3):1045–1052.10.1182/blood-2002-06-1761 [PubMed: 12393541]

Deans JP, Li H, Polyak MJ. CD20-mediated apoptosis: Signalling through lipid rafts. Immunology. 2002; 107(2):176–182.10.1046/j.1365-2567.2002.01495.x [PubMed: 12383196]

Duivenvoorden R, Tang J, Cormode DP, Mieszawska AJ, Izquierdo-Garcia D, Ozcan C, et al. A statin-loaded reconstituted high-density lipoprotein nanoparticle inhibits atherosclerotic plaque inflammation. Nat Commun. 2014; 5:3065–3075.10.1038/ncomms4065 [PubMed: 24445279]

Gerber HP, Koehn FE, Abraham RT. The Antibody-Drug Conjugate: An enabling modality for natural product-based cancer therapeutics. Nat Prod Rep. 2013; 30(5):625–639.10.1039/c3np20113a [PubMed: 23525375]

Ghosh M, Ryan RO. ApoE enhances nanodisk-mediated curcumin delivery to glioblastoma multiforme cells. Nanomedicine (Lond). 2014; 9(6):763–771.10.2217/nnm.13.35 [PubMed: 23879635]

Ghosh M, Singh ATK, Xu W, Sulchek T, Gordon LI, Ryan RO. Curcumin nanodisks: Formulation and characterization. Nanomedicine. 2011; 7(2):162–167.10.1016/j.nano.2010.08.002 [PubMed: 20817125]

Gordon LI, Bernstein SH, Jares P, Kahl BS, Witzig TE, Dreyling M. Recent advances in mantle cell lymphoma: report of the 2013 Mantle Cell Lymphoma Consortium Workshop. Leuk Lymphoma. 2014; 55(10):2262–2270.10.3109/10428194.2013.876634 [PubMed: 24512319]

Gupta SC, Prasad S, Kim JH, Patchva S, Webb LJ, Priyadarsini IK, Aggarwal BB. Multitargeting by curcumin as revealed by molecular interaction studies. Nat Prod Rep. 2011; 28(12):1937–1955.10.1039/c1np00051a [PubMed: 21979811]

Hagemeyer CE, von Zur Muhlen C, von Elverfeldt D, Peter K. Single-chain antibodies as diagnostic tools and therapeutic agents. Thromb Haemost. 2009; 101(6):1012–1019.10.1160/TH08-12-0816 [PubMed: 19492141]

Hussain AR, Ahmed M, Al-Jomah NA, Khan AS, Manogaran P, Sultana M, et al. Curcumin suppresses constitutive activation of nuclear factor-kappa B and requires functional Bax to induce apoptosis in Burkitt's lymphoma cell lines. Mol Cancer Ther. 2008; 7(10):3318–3329.10.1158/1535-7163.MCT-08-0541 [PubMed: 18852135]

Iovannisci DM, Beckstead JA, Ryan RO. Targeting nanodisks via a single chain variable antibody-apolipoprotein chimera. Biochem Biophys Res Commun. 2009; 379(2):466–469.10.1016/j.bbrc.2008.12.077 [PubMed: 19114030]

Lianos GD, Vlachos K, Zoras O, Katsios C, Cho WC, Roukos DH. Potential of antibody-drug conjugates and novel therapeutics in breast cancer management. Onco Targets Ther. 2014; 7:491–500.10.2147/OTT.S34235 [PubMed: 24711706]

Maloney DG, Grillo-Lopez AJ, White CA, Bodken D, Schilder RJ, Neidhart JA, et al. IDEC-C2B8 (Rituximab) anti-CD20 monoclonal antibody therapy in patients with relapsed low-grade non-Hodgkin's lymphoma. Blood. 1997; 90(6):2188–2195. [PubMed: 9310469]

Oda MN, Hargreaves P, Beckstead JA, Redmond KA, van Antwerpen R, Ryan RO. Reconstituted high density lipoprotein enriched with the polyene antibiotic amphotericin B. J Lipid Res. 2006; 47(2):260–267.10.1194/jlr.D500033-JLR200 [PubMed: 16314670]

Polyak MJ, Deans JP. Alanine-170 and proline-172 are critical determinants for extracellular CD20 epitopes; heterogeneity in the fine specificity of CD20 monoclonal antibodies is defined by additional requirements imposed by both amino acid sequence and quaternary structure. Blood. 2002; 99(9):3256–3262.10.1182/blood.V99.9.3256 [PubMed: 11964291]

Press OW, Eary JE, Appelbaum FR, Martin PJ, Nelp WB, et al. Phase II trial of I-131-B1 (anti-CD20) antibody therapy with autologous stem cell transplantation for relapsed B cell lymphoma. Lancet. 1995; 346(8971):336–340.10.1016/S0140-6736(95)92225-3 [PubMed: 7623531]

Redmond KA, Nguyen TS, Ryan RO. All-trans retinoic acid nanodisks. Int J Pharm. 2007; 339(1–2):246–250.10.1016/j.ijpharm.2007.02.033 [PubMed: 17412536]

Ryan RO. Nanodisks: hydrophobic drug delivery vehicle. Expert Opin Drug Deliv. 2008; 5(3):343–351.10.1517/17425247.5.3.343 [PubMed: 18318655]

Ryan RO. Nanobiotechnology applications of reconstituted high density lipoprotein. J Nanobiotechnology. 2010; 8:28.10.1186/1477-3155-8-28 [PubMed: 21122135]

Ryan RO, Forte TM, Oda MN. Optimized bacterial expression of humanapolipoproteinA-I. Protein Expr Purif. 2003; 27(1):98–103.10.1016/S1046-5928(02)00568-5 [PubMed: 12509990]

Scott SD. Rituximab: a new therapeutic monoclonal antibody for non-Hodgkin's lymphoma. Cancer Pract. 1998; 6(3):195–197.10.1046/j.1523-5394.1998.006003195.x [PubMed: 9652253]

Shan D, Press OW, Tsu TT, Hayden MS, Ledbetter JA. Characterization of scFv-Ig constructs generated from the anti-CD20 mAb 1F5 using linker peptides of varying lengths. J Immunol. 1999; 162(11):6589–6595. [PubMed: 10352275]

Shankar S, Chen Q, Sarva K, Siddiqui I, Srivastava RK. Curcumin enhances the apoptosis-inducing potential of TRAIL in prostate cancer cells: molecular mechanisms of apoptosis, migration and angiogenesis. J Mol Signal. 2007; 2:10.10.1186/1750-2187-2-10 [PubMed: 17916240]

Shen WJ, Hu J, Hu Z, Kraemer FB, Azhar S. Scavenger receptor class B type I (SR-BI): a versatile receptor with multiple functions and actions. Metabolism. 2014; 63(7):875–886.10.1016/j.metabol.2014.03.011 [PubMed: 24854385]

Shishodia S, Amin HM, Lai R, Aggarwal BB. Curcumin (diferuloylmethane) inhibits constitutive NF-kappaB activation, induces G1/S arrest, suppresses proliferation, and induces apoptosis in mantle cell lymphoma. Biochem Pharmacol. 2005; 70(5):700–713.10.1016/j.bcp.2005.04.043 [PubMed: 16023083]

Singh AT, Evens AM, Anderson RJ, Beckstead JA, Sankar N, Sassano A, et al. All *trans* retinoic acid nanodisks enhance retinoic acid receptor mediated apoptosis and cell cycle arrest in mantle cell lymphoma. Br J Haematol. 2010; 150(2):158–169.10.1111/j.1365-2141.2010.08209.x [PubMed: 20507312]

Singh ATK, Ghosh M, Forte TM, Ryan RO, Gordon LI. Curcumin nanodisk-induced apoptosis in mantle cell lymphoma. Leuk Lymphoma. 2011; 52(8):1537–1543.10.3109/10428194.2011.584253 [PubMed: 21699455]

Tedder TF, Engel P. CD20: a regulator of cell-cycle progression of B lymphocytes. Immunol Today. 1994; 15(9):450–454.10.1016/0167-5699(94)90276-3 [PubMed: 7524522]

Teeling JL, Mackus WJ, Wiegman LJ, van den Brakel JH, Beers SA, French RR, et al. The biological activity of human CD20 monoclonal antibodies is linked to unique epitopes on CD20. J Immunol. 2006; 177(1):362–371.10.4049/jimmunol.177.1.362 [PubMed: 16785532]

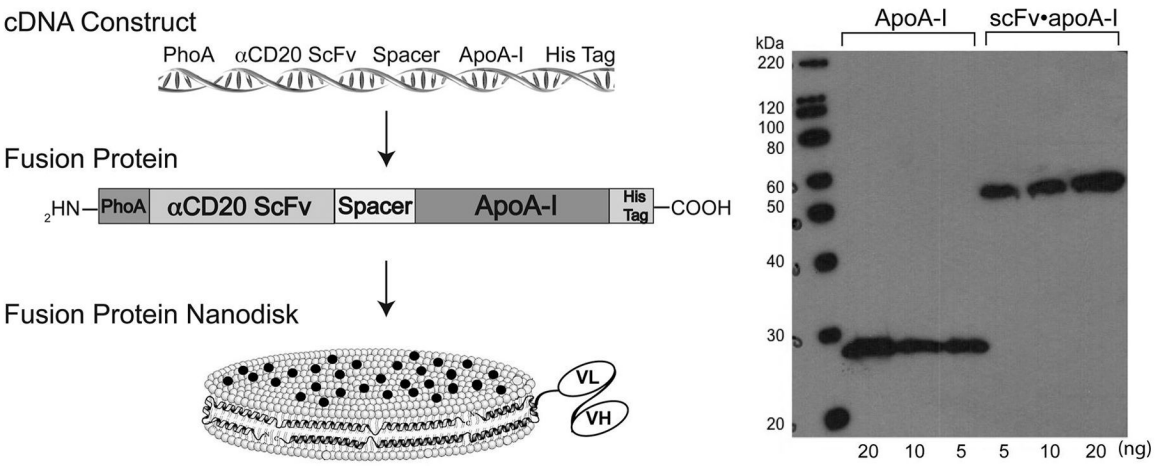

Fig. 1.

αCD20 scFv•apoA-I design, construction, expression and characterization. (Left) Schematic depicting αCD20 scFv•apoA-I chimera cDNA and protein. Also depicted is the fusion protein as the scaffold component of a ND (the black circles represent curcumin embedded in the phospholipid bilayer). (Right) SDS-PAGE immunoblot analysis of αCD20 scFv•apoA-I fusion protein. Samples were electrophoresed on a 4%–20% acrylamide gradient SDS slab gel under reducing conditions, transferred to PVDF membrane, and probed with anti-apoA-I. Left lane, molecular weight standards; center lanes, recombinant human apoA-I; right lanes, recombinant αCD20scFv•apoA-I fusion protein. Protein load (ng per well) are indicated.

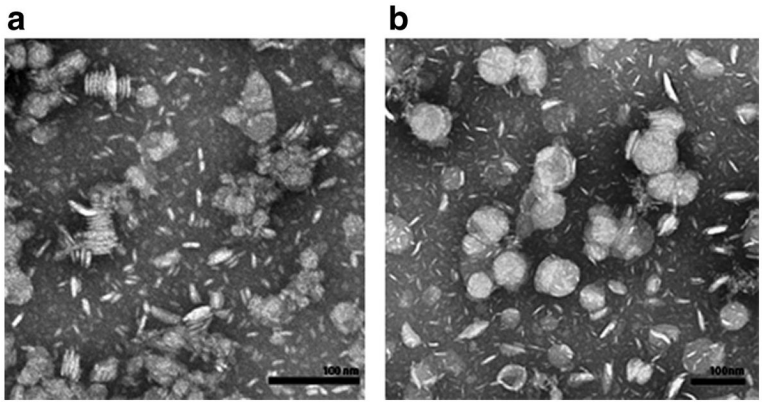

Fig. 2.

αCD20 scFv•apoA-I ND morphology with and without curcumin determined by negative stain electron microscopy. (*a*) αCD20 scFv•apoA-I ND without curcumin. (*b*) αCD20 scFv•apoA-I ND with curcumin. Bars represent 100 nm in each case.

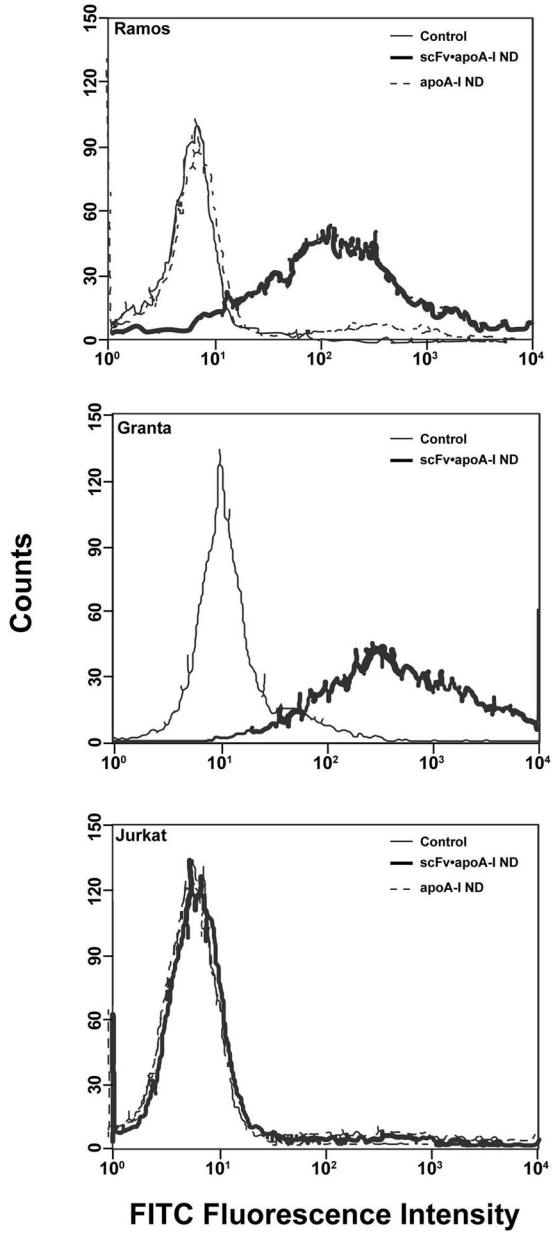

Fig. 3.

Specificity of αCD20 scFv•apoA-I ND binding to cells. ApoA-I ND or αCD20 scFv•apoA-I ND were incubated with Ramos (CD20-positive), Granta (CD20-positive), and Jurkat (CD20-negative) cells for 1 h at 37 °C and compared to control cells (PBS only). Binding was measured by FACS analysis using FITC-anti-apoA-I to detect the fusion protein. Representative scans are shown for Ramos (n = 3), Granta (n = 2), and Jurkat (n = 3) cells.

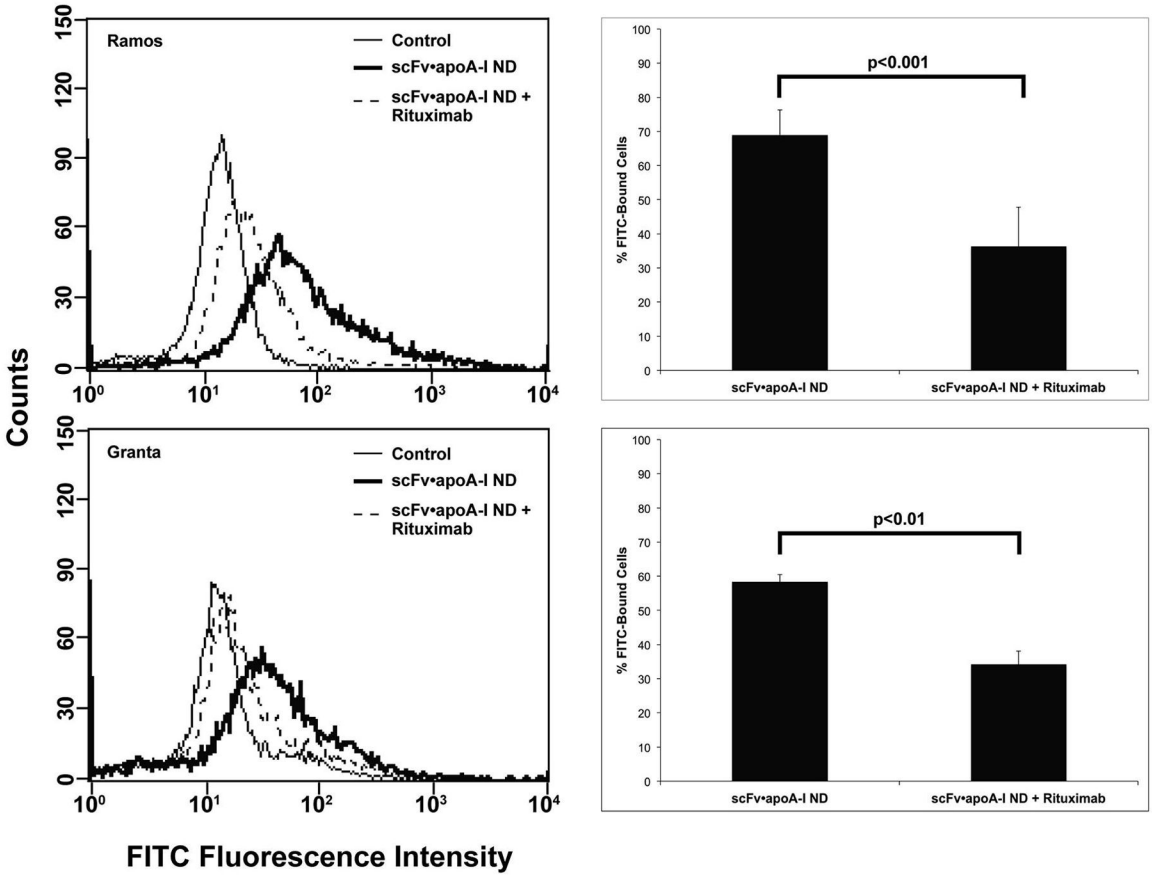

Fig. 4.

Effect of rituximab on αCD20 scFv•apoA-I ND binding to B lymphoma cells in culture. Ramos and Granta cells were incubated in the presence or absence of rituximab for 45 min at 4 °C. After washing to remove unbound rituximab, the cells were incubated with αCD20 scFv•apoA-I ND. Cell-associated scFv•apoA-I was detected by FACS after incubation with a FITC labeled anti-apoA-I. Scans for each cell line are representative of 3 experiments. Incubation of αCD20 scFv•apoA-I ND without rituximab treatment is shown as broad black line. Histograms show the percent change in cell binding after rituximab treatment. Significance between rituximab treated and untreated cells is indicated.

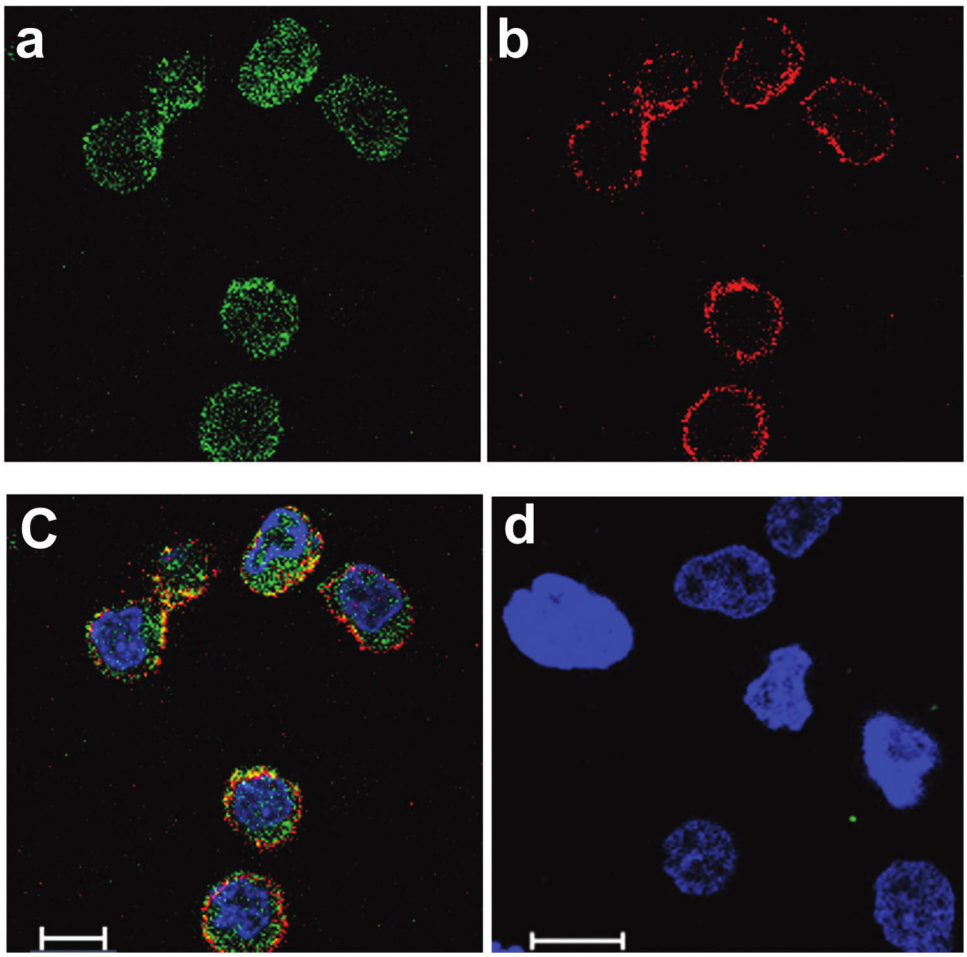

Fig. 5.

(Colour online) Confocal fluorescence microscopy of Granta cells following incubation with curcumin-loaded scFv•apoA-I ND. Curcumin was selected because its intrinsic fluorescence recorded between 493–630 nm following excitation at 488 nm expedites cellular localization. On the other hand, Alexa Fluor 680 labeled secondary antibody that recognizes the fusion protein was used to report on fusion protein distribution. Granta cells were incubated with 20 μmol/L curcumin-scFv•apoA-I ND for 1 h at 37 °C and washed to remove unbound scFv•apoA-I ND. (*a*) Curcumin fluorescence was detected in the green spectral region and is observed in the cytoplasm. (*b*) scFv•apoA-I ND protein moiety was detected with goat anti-apoA-I antibody and an Alexa Fluor 680 labeled anti-goat secondary antibody that fluoresces in the red spectral region. The fusion protein localizes to the cell surface. Panel (*c*) is a merged image for the Granta cells; the image suggests that some curcumin remains on the surface together with the protein (yellow fluorescence). (*d*) A merged image for CD20-negative Jurkat cells treated with curcumin-scFv•apoA-I ND included as a negative control. Hoechst 33342 was used to stain the cell nuclei. Scale bar: 10 μm.

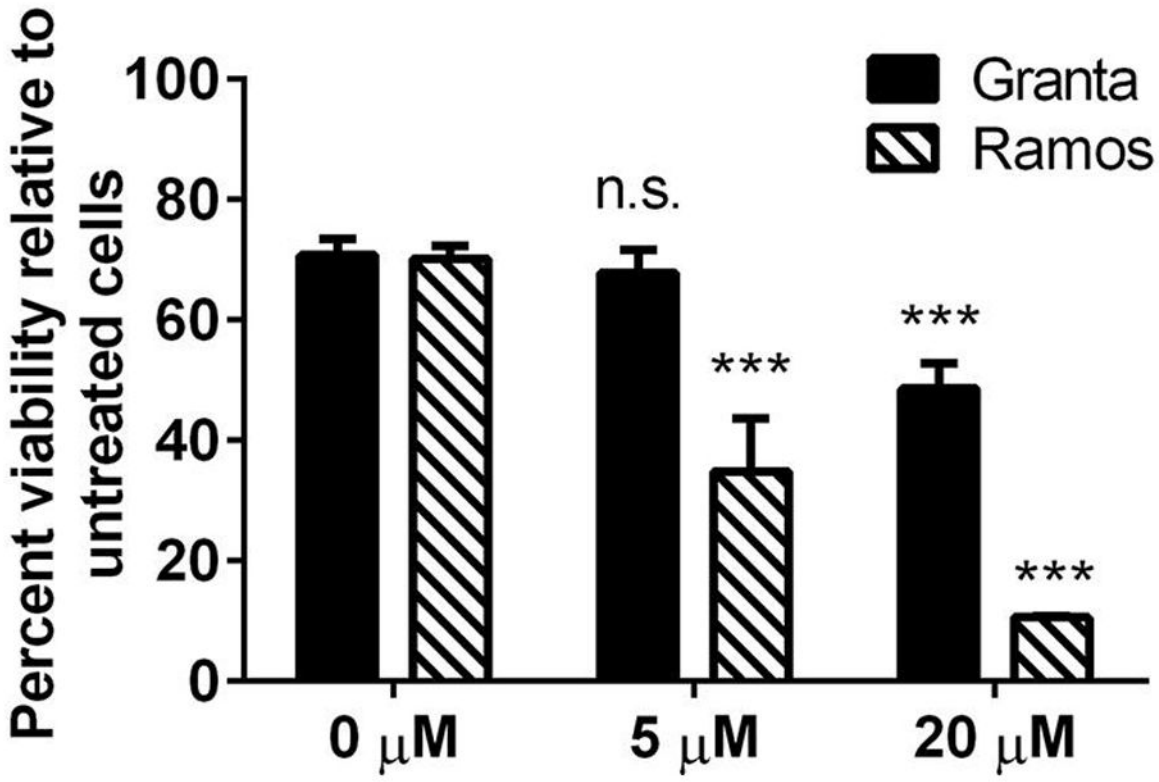

Fig. 6.

Effect of curcumin-loaded scFv•apoA-I ND on the viability of cultured B lymphoma cells. Ramos and Granta cells were incubated with empty scFv•apoA-I ND (0 μmol/L curcumin) and curcumin-scFv•apoA-I ND (5 and 20 μmol/L curcumin) for 48 h. Cell viability was determined using the MTT assay according to manufacturer's instructions. Values are mean ± SEM ($n = 4$). ***$P < 0.001$, n.s. = not significant, compared to cells without curcumin.